PRIFYSGOL
BANGOR
UNIVERSITY

Photonic Millimeter Wave Generation and Stabilization in Optically Injected Discrete-mode Semiconductor Lasers subject to Photonic Filter Feedback

Zhong, Z. Q.; Chang, Da; Chen, J. J.; Feng, S.D.; Tao, C.Y.; Jin, Wei; Jiang, Shan; Hong, Yanhua

Journal of Lightwave Technology

Photonic Millimeter Wave Generation and Stabilization in Optically Injected Discrete-mode Semiconductor Lasers subject to Photonic Filter Feedback

Z. Q. Zhong, D. Chang, J. J. Chen, S. D. Feng, C. Y. Tao, W. Jin, S. Jiang, and Y. H. Hong[*]

Abstract—**Photonic millimeter wave signal generation and stabilization based on nonlinear dynamics of optically injected discrete-mode semiconductor lasers with photonic filter feedback are experimentally and numerically studied. The photonic filter is constructed by jointing two ports of a 2×2 optical coupler to form a ring cavity recirculation and is modelled as an infinite impulse response filter. The results show that >30GHz photonic millimeter wave signals can be obtained after optical to electrical conversion of the period-one oscillation output of the optically injected discrete-mode semiconductor laser. More importantly, the linewidth, side peak suppression ratio, as well as the stability of the generated millimeter wave, can be optimized using the photonic filter feedback. A fair comparison of the photonic filter feedback scheme and the single/double optical feedback schemes in terms of optimization performance has been made. The corresponding results demonstrate that the photonic filter feedback scheme has obvious superiority in millimeter wave side peak suppression and stability. The effect of the coupling coefficient as well as the phase variables in the ring cavity has also been discussed in the simulation work and the results qualitatively agree with the experimental observations.**

Index Terms—**Microwave photonics, millimeter wave generation and stabilization, discrete mode semiconductor laser, photonic filter feedback**

I. INTRODUCTION

The spectrum shortages in the radio/microwave frequency band drive both industry and academia to explore higher frequency ranges. Consequently, millimeter wave (mmWave) signals have been considered as a core enabler in the envisioned future for communications, autonomous driving, medical treatment, and radar sensing systems [1]. Compared with microwave based application in communications, the mmWave frequencies can support higher bandwidth and increased capacity, allowing for faster data transfer and low latency scenarios [2]. Moreover, the higher directionality of mmWave allows for more focused transmission [3] resulting in less susceptible to be eavesdropped and improved security. In addition, antennas for mmWave devices can be miniaturized, [4], thus many future portability scenarios are expected to be realized based on mmWave signals. However, mmWave has not yet widely deployed in commercial communications because some technical challenges still need to be solved. One challenge is the high losses and weak diffraction when mmWave signals are transmitted, and the second is to generate narrow linewidth and highly stable high-frequency mmWave signals. As the generation of mmWave signals by conventional electronic circuits has limitations in cost-effectiveness, a photonic synthesis approach has been utilized to overcome the difficulties of mmWave signal generation [5]. Photonic mmWave generation offers superior benefits such as the ability to generate higher frequency bands, a wider range of frequency tunability, minimal loss and strong resistance to electromagnetic interference when transmitted through optical fibers [6]. Therefore, photonic mmWave generation has been a hot research topic and attracted extensive attention in recent years [7]–[28].

Semiconductor lasers (SLs) are considered as promising coherent light sources for photonic microwave and mmWave generation systems due to power efficiency and highly reliable, thus many schemes have been proposed and demonstrated in generating photonic microwave and mmWave signals, which include optical heterodyne [7]–[9], direct and external modulation [10], [11], mode-locked [12], optoelectronic oscillator [13]–[15] and period one (P1) oscillation of SLs [16]–[28]. Among these schemes, the nonlinear dynamical P1 oscillation of optically injected SLs has unique advantages such as the simple structure, because the limit cycle oscillation can be easily obtained from the Hopf bifurcation by suitable optical injection [16]. Furthermore, due to the injection pulling and the red-shifting effect [17], the frequency of the generated signal can be significantly increased and flexibly tuned compared with the original relaxation resonance frequency of SLs. Nevertheless, the microwave/mmWave signals generated through the P1 dynamics of optically injected SLs usually

Z. Q. Zhong, S. D. Feng and C. Y. Tao are with the College of Science, Chongqing University of Technology, Chongqing 400054, China. (Email: zqzhong@cqut.edu.cn)

D. Chang, W. Jin, S. Jiang, and Y. H. Hong are with the School of Computer Science and Electronic Engineering, Bangor University, Bangor, LL57 1UT, UK. (Email: y.hong@bangor.ac.uk)

J. J. Chen is with School of Medical Engineering and Technology, Xinjiang Medical University, Ürümqi 830011, China (Email: cjjliyan@163.com)

suffer from poor 3-dB linewidth, primarily caused by the spontaneous emission noise of the injected laser [18] and the frequency jitter due to the variations in optically injected frequency and power [19]. To mitigate the abovementioned obstacles, several stabilization techniques for P1 nonlinear dynamics have been proposed and could be typically classified into pure electronic stabilization [20], [21], all-optical stabilization [22]–[24] and optoelectronic hybrid stabilization approaches [25]–[28]. For pure electronic stabilization approaches, an electronic radio or microwave frequency signal is usually utilized as a reference to modulate the DC bias current of the optically injected slave laser. Simpson et al. experimentally demonstrated tunable 9.5 to 17.1 GHz photonic microwave signals with a linewidth below 1 kHz by locking the P1 oscillation frequency to the direct modulation frequency [20]. Fan et al. proposed the high order subharmonic double-locking technique, which utilizes 1/n of the P1 oscillation frequency electronic signals to lock and stabilize the photonic microwave and mmWave signals [21]. For all-optical stabilization approaches, delayed optical feedback schemes are widely adopted due to their easy implementation and cost-friendliness. The mechanism is that the delayed optical signals lock the P1 oscillation of the slave lasers. Lo et al. numerically demonstrated that optical feedback can effectively stabilize the period-one dynamics, thereby significantly reducing microwave linewidth and phase noise [22]. Zhuang et al. theoretically clarified the stabilization mechanism of single and double optical feedback in distributed feedback (DFB) lasers [23]. We experimentally reported the effect of delayed optical feedback on the stability and linewidth of the generated photonic microwave in vertical-cavity surface-emitting lasers (VCSELs) [24]. For optoelectronic hybrid stabilization approaches, optoelectronic feedback [25], [26] and modulated optical injection [27], [28] schemes are widely adopted. In the optoelectronic feedback schemes, Ma et al. experimentally achieved 3-dB linewidth of <1kHz microwave signals in a microdisk laser [25]. Suelzer et al. experimentally obtained six orders of magnitude reduction in the microwave linewidth without electronic filters or amplifiers in the optoelectronic feedback loop [26]. In the modulated optical injection schemes, a continuous wave optical signal modulated by a phase modulator driven by a strong high-purity electronic microwave synthesizer, generates an optical signal with multiple highly corrected modulation sidebands to injection lock and stabilize the P1 oscillation [27], [28]. Overall, the abovementioned stabilization approaches have their own advantages in obtaining high frequency, narrow linewidth, and low phase noise microwave, and should be comprehensively considered in practical applications.

Discrete-mode (DM) semiconductor lasers possess a similar physical structure as conventional Fabry-Perot lasers but contain a limited number of etched features along the ridge waveguide [29]. This distinguishing characteristic ensures DM lasers exhibit single longitudinal mode operation with high sidemode suppression. DM lasers are less sensitive to external perturbation, but they also show various nonlinear dynamics when they are subject to external perturbation [30]–[36], which

have attracted significant research interest. Broadband chaos, intermittent dynamics switching, optical frequency comb generation and random number generation based on nonlinear dynamics of the DM laser have been reported [30]–[36]. Microwave photonic signal generation in optically injected DM lasers has also been preliminarily studied [35]. To further exploit the potential of DM lasers in photonic mmWave generation, in this paper, optical injection with large frequency detuning is applied and the photonic filter feedback is introduced to optimize the generated mmWave signals. The photonic filter feedback is achieved through an optical ring cavity, which is constructed by connecting two ports of an optical coupler [37]. This ring cavity structure is also known as an infinite impulse response single-source microwave photonic filters (IIR SSMPFs) or fiber ring resonators. Such configuration has been adopted to generate wide band chaotic signals [38], reshape the spectral profile and suppress the time delay signature of chaos [39], [40]. Besides, self-injection locking to an external fiber cavity has been experimentally demonstrated to control and tune the laser linewidth [41] thus it is worth exploring the effect of such photonic filter feedback on the quality of photonic mmWave signals.

Consequently, we focus on the photonic mmWave signal generation based on the P1 dynamics of optically injected DM laser and enhancing the quality of the generated mmWave signal by photonic filter feedback. In the experimental work of Section II, the linewidth, side peak suppression ratio, and stability of the generated mmWave are investigated. A comparison between the photonic filter feedback scheme and single/double optical feedback scheme on the linewidth reduction, side peak suppression and stability has been conducted and analyzed. In the theoretical work of Section III, the photonic filter is modelled, and the corresponding mechanism of improving the quality of the photonic mmWave signal is further analyzed and explained.

II. EXPERIMENTAL SETUP AND RESULTS

This section focuses on the experimental studies on the photonic mmWave generation based on the P1 dynamics of optically injected DM lasers and the quality enhancement by photonic filter feedback. The linewidth, side peak suppression (SPS) ratio and stability of the generated millimeter wave signals are inspected and the optimization performance of single optical feedback, double optical feedback, as well as photonic filter feedback is compared. In addition, the effect of feedback strength and the coupling coefficient of the photonic filter on the generated mmWave signal are investigated.

A. Experimental Setup

The experimental setup diagram is shown in Fig. 1. A commercially available DM laser (EP1550-DM-01-FA, Eblana Photonics) is used as the slave laser. A low noise current source (YOKOGAWA, GS200) is utilized to provide a bias current of 40 mA, which is 1.8 times of the threshold current of the DM laser when the temperature is stabilized at room temperature by a high accuracy temperature controller (Tektronix, TED 200). Under this condition, the lasing wavelength of free-running

DM laser is about 1548.23 nm and the output power is 1.6 mW. A tunable laser source (Agilent 8164A) is used as the master laser. The emission of the master laser injects into the slave laser after passing through a polarization controller (PC1), a 50: 50 fiber coupler (FC1) and an optical circulator (OC). The polarization of the injected beam is aligned by PC1. The output of the slave laser first passes through the OC and then divided by FC2 into two paths. One path of FC2 is sent to the detection system. After an optical-to-electrical conversion, the electrical spectra of the slave laser output are recorded by an electrical spectrum analyzer (R&S FSW43). The other path constitutes a feedback loop, which includes PC2, a variable attenuator (VA), the photonic filter, FC1 and OC. The photonic filter is constructed by connecting ports 2 and 4 of FC3 and has been discussed in detail in [37]. The optical feedback power can be adjusted by VA.
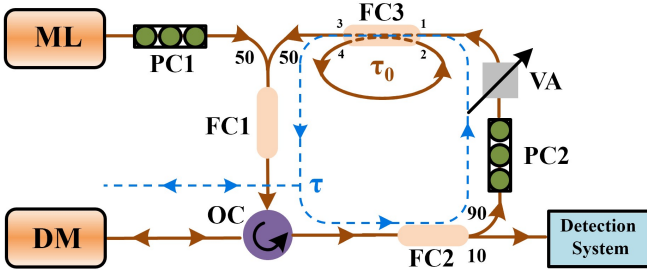

Fig. 1 Experimental setup. ML: master laser, DM: discrete-mode laser, PC: polarization controller, FC: fiber coupler, OC: optical circulator, VA: variable attenuator.

In this paper, the optical injection ratio is defined as the ratio of the injection power to the output power of the solitary slave laser. The injection power is measured before the injection beam enters the slave laser. The frequency detuning is defined as the difference of the injection optical frequency from the free-running optical frequency of the DM laser. The optical feedback power is measured at port 3 of FC3, but the loss of FC1 and OC as well as the split ratio have been taken into account in the calculation of the feedback strength, therefore, the feedback strength is equivalent to the power of the feedback beam before entering the DM laser. The coupling coefficient of the ring cavity is defined as a percentage of the power transferred from port 1 to port 3 in FC3, as shown in Fig. 1.

B. Experimental Results

The photonic mmWave is first generated after optical to electrical conversion from the period-one oscillation of the optically injected DM laser with an optical injection ratio of 0.7 and frequency detuning of 30 GHz. As shown in Fig. 2(a), the frequency is offset at the fundamental frequency of 31.8 GHz, which is generated by the beating of the regenerated injection frequency and the red-shifted cavity resonant frequency. With the resolution bandwidth of 20 kHz and sweep time of 5 ms, the 3-dB linewidth of the generated photonic mmWave is measured to be 1.95 MHz. Such a linewidth level is not suitable for most of the abovementioned application scenarios. For this reason, introducing stabilization approaches are required for generating high-quality mmWave. In this paper, a photonic filter feedback scheme is utilized to improve the quality of the

generated mmWave signal. For comparison, the effect of widely used single optical feedback and double optical feedback schemes are also applied. The corresponding generated mmWave power spectra are illustrated in Fig. 2(b-d).
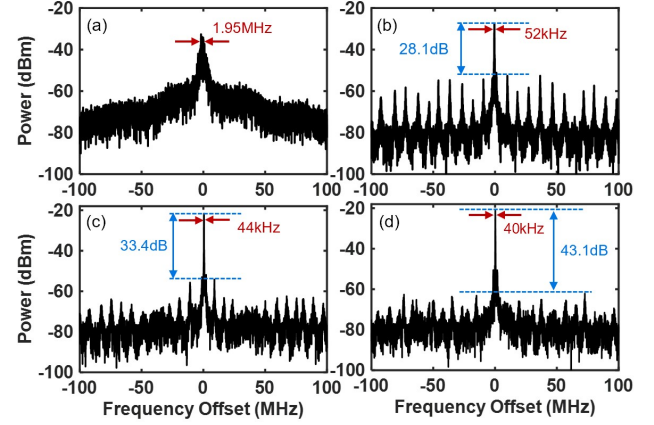

Fig. 2 Power spectra of the optically injected DM laser output when it is driven into P1 oscillation (a) without feedback, (b) with single optical feedback, (c) with double optical feedback, (d) with photonic filter feedback. The optical injection ratio and frequency detuning are fixed at 0.7 and 30 GHz, respectively. The feedback strength keeps at -22 dBm for (b)-(d).

For a fair comparison, the optical injection parameters in Fig. 2(b-d) are the same as those in Fig. 2(a). For the single optical feedback case, FC3 in Fig. 1 is replaced by a 2 m optical fiber patch cable to keep the optical feedback length to be comparable with the photonic filter feedback length. As shown in Fig. 2(b), when the feedback strength is set at -22 dBm, the fundamental frequency f_0 has shifted slightly to 31.3 GHz and the linewidth has reduced to 52 kHz. However, numerous residual side peaks emerged equally spaced of approximately 9.5 MHz, which is close to the reciprocal of the feedback delay time of 105 ns. This phenomenon is similar to that observed in the DFB laser or VCSELs. To quantify the relative strength of the side peaks in the power spectrum, the side peak suppression (SPS) ratio is introduced and defined as the ratio of the power at the fundamental frequency to the maximum power of the side peaks [35]. Accordingly, the SPS ratio of the single optical feedback case is 28.1 dB. On the basis of single feedback scheme, another optical fiber patch cable with one meter length is added for the double optical feedback configuration [17] and the feedback strength for each loop is set identically, which is half of the feedback strength used in single optical feedback case. All these settings are to ensure the double optical feedback scheme can effectively suppress the side peaks while maintaining a low phase variance of the generated mmWave [23]. As a result, shown in Fig. 2(c), the 3-dB linewidth of the generated photonic mmWave is further reduced to 44kHz and the SPS ratio of the mmWave increases to 33.4 dB. The suppression of the residual side peaks in double feedback scheme is due to Vernier effect caused by the slightly different time delay of two feedback loops [42], which has also been experimentally observed in DFB lasers [23] and VCSELs [24]. Finally, the mmWave power spectrum when photonic filter feedback is presented in Fig. 2(d). The feedback strength is the same as that of the single optical feedback case. FC3 here is a

10:90 fiber coupler and 90% optical power is coupled to the ring cavity constructed by connecting ports 2 and 4 of FC3, therefore, the coupling coefficient is 0.1. As shown in Fig. 2(d), the 3-dB linewidth of the generated photonic mmWave further reduces to 40 kHz. More importantly, the SPS ratio of the generated mmWave signal has a 9.7 dB (15 dB) improvement in comparison with the double (single) optical feedback case. The mechanism can be explained by the fact that jointing port 2 and port 4 of FC3 provides a basic delay for each cavity recirculation, which could be regarded as an infinite impulse response filter. Each cavity recirculation delivers external optical feedback with different feedback strengths and delay times according to the coupling coefficient of FC3 and the count of recirculation. As such, the feedback delay is lengthened to some extent, which is beneficial to phase noise reduction [22]. Moreover, the multiple external cavity modes induced by incommensurate optical feedback can match each other's frequency following Vernier principle [42]. Therefore, the residual side peaks become contiguous and suppressed, resulting in a significant phase variance reduction.
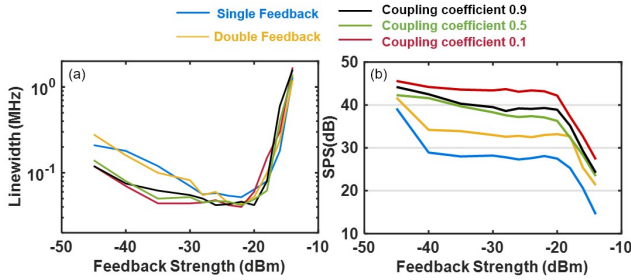

Fig. 3 Millimeter wave linewidth (a) and side peak suppression ratio (b) as a function of optical feedback strength.

Next, the effect of the feedback strength on the mmWave linewidth as well as the SPS ratio is explored. For comparison, the single optical feedback, double optical feedback and the photonic filter with three coupling coefficients are considered to evaluate the quality of the generated mmWave. Fig. 3 shows the linewidth and SPS versus the feedback strength. The parameters in Fig. 3 are the same as those used in Fig. 2 except for the feedback strength. As illustrated in Fig. 3(a), the evolutions of mmWave linewidth as a function of optical feedback strength for all configurations have similar trends. When the optical feedback is increased, the linewidth of the generated mmWave signal initially decreases and reaches a minimum value. However, further increasing the feedback strength results in a subsequent increase in the linewidth due to the destruction of P1 oscillation. The DM laser will enter a quasi-periodic or chaotic state under strong feedback strength, so the maximal feedback strength should be limit [22]. Compared with only optical injection configuration, optical feedback can reduce the linewidth of the mmWave by at least an order of magnitude. Particularly the photonic filter feedback outperforms single optical feedback and double optical feedback in reducing mmWave linewidth for relatively weak feedback strength (<-30dBm). Given that the residual mmWave side peaks, revealing the external cavity modes, leading to phase variance degradation, high SPS ratio and

narrow linewidth are acquired in P1 dynamic based photonic mmWave generation. Fig. 3(b) shows that for single optical feedback, the SPS ratio starts to decrease quickly when the feedback strength increases from -45 dBm to -40 dBm, then the SPS ratio curve keeps almost flat with a value of about 27.5 dB until the feedback strength reaches about -20 dBm. The flat SPS ratio over a wide range of the feedback strength may result from the filtering effect caused by the special structure of the DM laser, and its physical mechanism remains to be further investigated. Further increasing the feedback strength results in a rapid decrease of SPS ratio due to the feedback induced dynamics switching. These results are similar to our previous work [35]. In order to obtain a higher SPS ratio of the generated mmWave, the double optical feedback scheme is adopted. The corresponding SPS ratio as a function of optical feedback strength is marked as the yellow curve in Fig. 3(b). Similar to the single optical feedback case, the SPS ratio of the double optical feedback configuration first decreases with increasing feedback strength at the feedback strength < -40 dBm, and then stabilizes at about 33 dB over a feedback range of about 20 dB. Further increasing the optical feedback strength, the SPS ratio decreases rapidly again. The SPS ratio of the double optical feedback have an average of 5.5 dB enhancement compared with those of single feedback configuration. Finally, for the photonic filter scheme, the coupling coefficients are set as 0.9, 0.5, and 0.1, corresponding to 10% (low), 50% (median) and 90% (high) optical power propagating in the ring cavity of the photonic filter. As shown in Fig. 3(b), for 0.9 and 0.5 coupling coefficients, the coupling coefficient of 0.9 performs better than the coupling coefficientn of 0.5 in enhancing the SPS ratio, but the trend is very similar. On the other hand, for the coupling coefficient of 0.1, i.e. most optical power enters the ring cavity of the photonic filter, the residual side peaks are contiguous and suppressed due to Vernier effect of multiple cavity recirculation, thus the SPS ratio of the generated millimeter wave can be maintained at about 43 dB over a wide feedback strength. Compared with single and double optical feedback approaches, the photonic filter feedback configuration can achieve a higher SPS ratio whilst maintaining competitive narrow linewidth performance.
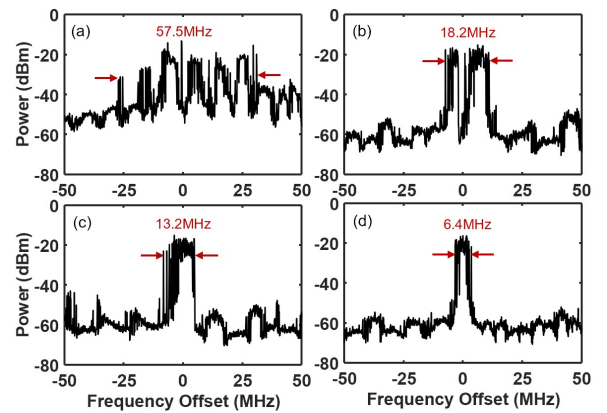

Fig. 4 Power spectra of the optically injected DM laser output when the sweep time of the electrical spectrum analyzer is set at 30 seconds (a) without feedback, (b) with single optical feedback, (c) with double optical feedback, (d) with photonic filter feedback.

It should be pointed out that, the mmWave fundamental frequency peaks depicted in Fig. 2(a) do not consistently appear at the center of the frequency span due to the fluctuations of the P1 fundamental frequency. In practical terms, the fundamental frequency peaks inevitably appear within a certain frequency range because of the noise from DM laser's bias current and temperature controller even if the injection parameters are held constant. Therefore, the stability of the generated mmWave is another worthwhile research in the experimental work. To quantitative analyze the stability, the sweep time of the electrical spectrum analyzer is set to 30 seconds, which allows it to capture multiple fundamental frequency peaks and display a single image over this period of timeframe. As such the fluctuation range of the fundamental frequency peak can represent the stability of the generated mmWave, the narrower fluctuation ranges the better stability performance. In Fig. 4, all parameters are the same as those in Fig. 2 apart from the sweep time of the electrical spectrum analyzer. As shown in Fig. 4(a), without optical feedback stabilization, the location of the fundamental frequency peak appears within 57.5 MHz. When single optical feedback is introduced, the fluctuation range decreases to 18.2 MHz shown in Fig. 4(b). For double feedback configuration, the fluctuation range of the fundamental frequency peak reduces to 13.2 MHz, which demonstrates double optical feedback scheme can further stabilize the mmWave frequency. Similar results have also been reported in VCSELs [24]. Finally, when photonic filter feedback is introduced, as shown in Fig. 4(d), the fluctuation region further reduces to 6.4 MHz, which is about half of the fluctuation range with the double feedback configuration. In addition, the side peaks become contiguous and suppressed. All the above results indicate that photonic filter feedback not only possesses excellent SPS performance but also has a distinctive advantage in stabilizing the fundamental frequency of the generated mmWave. The advantages of photonic filter feedback may be due to the nature of its multi-cavity feedback and a small fraction of feedback with very long feedback cavity length, and the physical mechanism behind the better stability of photonic filter feedback needs to be further studied in detail in the future.

III. THEORETICAL MODEL AND RESULTS

In this section, the photonic mmWave generation and its quality improvement in an optically injected DM laser are numerically studied. It is proposed to consider the nonlinear carrier recombination as well as the Gaussian white noise in both electric field and carrier in the theoretical model for optically injected DM laser. In addition, the model also takes into account the feedback term from the photonic filter. The corresponding quality of the generated mmWave is fairly compared with those of single and double optical feedback configurations.

A. Theoretical Model

As mentioned above, the model in [43] can be used to simulate the optically injected DM laser with optical feedback configuration and the nonlinear carrier recombination as well

as the Gaussian white noise in both electric field and carrier are also considered [36].

$$\frac{dE(t)}{dt} = \frac{(1+i\alpha)}{2}\left[\frac{g(N-N_0)}{1+\varepsilon|E(t)|^2} - \frac{1}{\tau_p}\right]E(t) + \kappa E_{inj}e^{i2\pi\Delta ft} + E_{fb} + \sqrt{\beta BN}\xi(t) \quad (1)$$

$$\frac{dN(t)}{dt} = \frac{I}{e} - (AN + BN^2 + CN^3) - \frac{g(N-N_0)|E(t)|^2}{1+\varepsilon|E(t)|^2}$$
$$+ \sqrt{2\left(AN + BN^2 + CN^3 + \frac{I}{e}\right)}\xi_N - 2\sqrt{\beta BN}(E_r\xi_r + E_i\xi_i) \quad (2)$$

where $E(t) = E_r + iE_i$ represents the slowly varying complex electric field, E_r and E_i are its real and imaginary parts, respectively. $N(t)$ is the carrier number in the active region. α is the linewidth enhancement factor, g is the differential gain coefficient, N_0 is the transparency carrier number and ε is the gain saturation factor, τ_p is the photon lifetime, κ represents the injection strength, E_{inj} is the injection field amplitude, Δf is the frequency difference between the master and the solitary DM laser, namely frequency detuning. I is the bias current, e is the electron charge, A, B, and C are the non-radiative, spontaneous, and Auger recombination coefficient, respectively. For the noise terms, the spontaneous emission rate is given by $R_{sp}(N) = \beta BN^2$, β is the fraction of spontaneous emission coupled into the lasing mode, $\xi(t) = \xi_r + i\xi_i$ is the complex Gaussian white noise with zero average and correlation given by $<\xi(t)\,\xi^*(t')> = \delta(t-t')$ where $\delta(t)$ is the Dirac delta function. In addition, carrier noise is also considered for describing statistics in semiconductor laser dynamics [36] and ξ_N represents the real Gaussian white noise of zero average and correlation given by $<\xi_N(t)\,\xi_N(t')> = \delta(t-t')$, which is independent of the complex $\xi(t)$.

For the optical feedback term E_{fb}, the photonic filter can be characterized as an infinite impulse response photonic filter [37]. Therefore, the photonic filter feedback term can be described as,

$$\eta\left\{\sqrt{r}E(t-\tau)e^{-i\omega\tau} + \sum_{n=1}^{\infty}\left[\sqrt{r^{n-1}(1-r)^2}E(t-\tau-n\tau_0)e^{-i[\omega(\tau+n\tau_0)+\varphi]}\right]\right\} \quad (3)$$

Where η denotes the optical feedback strength, r is the coupling coefficient defined in the experiment, τ is the delay time of the optical feedback loop without considering the delay from the fiber ring resonator, shown in Fig.1. ω is the angular frequency of the DM laser, τ_0 is the delay time for one ring cavity recirculation, φ represents the phase variables in the ring cavity. To compare the optimization performance of different optical feedback schemes, single optical feedback and double optical feedback are investigated as well, which can be defined as $E_{fb-single} = \eta_s E(t-\tau_s)e^{-i\omega\tau_s}$ for single optical feedback scheme and $E_{fb-double} = \eta_1 E(t-\tau_1)e^{-i\omega\tau_1} + \eta_2 E(t-\tau_2)e^{-i\omega\tau_2}$ for double optical feedback scheme. The DM laser parameters are set as follows [35], where $\alpha = 3$, $g = 1.48 \times 10^4\,s^{-1}$, $N_0 = 1.93 \times 10^7$, $\varepsilon = 7.73 \times 10^{-8}$, $\tau_p = 2.17$ ps, $I = 30$ mA, $A = 2.8 \times 10^8\,s^{-1}$, $B = 9.8\,s^{-1}$, $C = 3.84 \times 10^{-7}\,s^{-1}$ and $\beta = 1.0 \times 10^{-6}$. Eqs. (1) and (2) are numerically solved by the second-order Runge-Kutta algorithm. The calculation uses a fixed step size of 2 ps and about 4 ms time duration thus the spectrum resolution is about 0.24kHz.
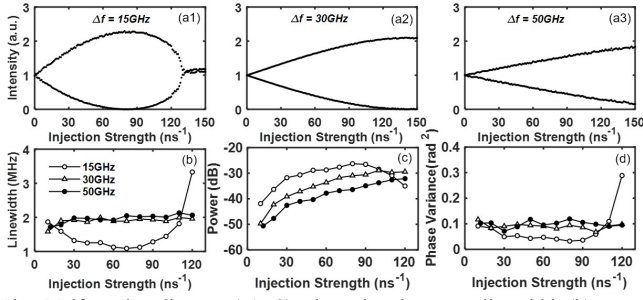
B. Theoretical Results and Analysis

Fig. 5 Bifurcation diagram (a1-a3), photonic microwave linewidth (b), power (c), and phase variance (d) of the DM laser output as a function of injection strength κ.

Firstly, the bifurcation and the generated microwave/mmWave properties as a function of injection strength κ are illustrated in Fig. 5. The bifurcation diagrams are plotted by extracting the maxima and minima of the time traces as a function of the injection strength, which can graphically represent the dynamical behavior when the injection strength is varied. Here the optical feedback is not introduced yet. For Δf = 15 GHz, as shown in Fig. 5(a1), with the increase of injection strength, P1 oscillation is invoked in the optically injected DM laser. The amplitude of the DM laser output oscillation gradually increases with the increase of the injection strength until κ reaches about 80 ns^{-1}, and the oscillation amplitude reaches its maximum value. Continue increasing the injection strength, the oscillation amplitude begins to drop until the injection strength reaches about 130 ns^{-1}. After that when $\kappa >$ 130 ns^{-1}, the DM laser is stably locked due to crossing the Hopf bifurcation point. When the frequency detuning increases to 30 GHz, as shown in Fig. 5(a2), the P1 oscillation amplitude monotonically increases with the increase of the injection strength until the injection strength extends to about 120 ns^{-1}. Further increasing the injection strength, the oscillation amplitude shows saturation. When the frequency detuning increases further to 50 GHz, as shown in Fig. 5(a3), the P1 oscillation amplitude grows monotonically within 150 ns^{-1} injection strength range because the Hopf bifurcation point shifts for the large frequency detuning. Similar results also have been reported in other optically injected semiconductor lasers [24], [44]. For the generated microwave signals, the linewidth is calculated using Lorentzian fitting and displayed in Fig.5(b). It can be found that for Δf = 15 GHz, the linewidth of the generated microwave signal achieves a minimum value of 1.1 MHz when κ = 70 ns^{-1}, continue to increase the injection strength, the linewidth of the generated microwave begins to increase again until the DM laser is stably locked. However, for larger frequency detuning Δf, the linewidth of the generated mmWave signals slowly increases with the increase of the injection strength. The linewidth for Δf = 50 GHz is slightly larger than that for Δf = 30 GHz but still stays around 2 MHz when injection strength increases to 120 ns^{-1}. In the simulation, the power of the generated mmWave signals is also calculated and defined as the peak power of the fundamental frequency. The corresponding power evolutions in Fig.5(a1-a3) are shown in Fig. 5(c). For the injection strength of $\kappa <$ 90 ns^{-1}, the power

of the generated microwave signals with the frequency detuning of Δf = 15 GHz is about 10dB stronger than that of the generated microwave/mmWave signals with Δf = 50 GHz, and the curve of mmWave power with Δf = 30 GHz is between those with Δf = 15 GHz and Δf = 50 GHz. In addition, the phase variance of the generated microwave/mmWave signals is calculated by integrating the 3 MHz to 1 GHz range single sideband of the power spectrum to the normalized mmWave power, which can also reveal the timing jitter characteristics of the generated mmWave signals [23]. The relationship between the phase variance and the injection strength in Fig.5(d) is similar with that of the linewidth in Fig.5(b). For Δf = 15 GHz, the minimum phase variance is 0.03 rad^2 at κ = 80 ns^{-1}; for 30 GHz and Δf = 50 GHz, the phase variance curves fluctuate near 0.1 rad^2 within 10 ns^{-1} to 120 ns^{-1} injection strength range. As the mmWave signals are the focus of this paper, the following discussion will be concentrated on the mmWave signals generated with Δf = 50 GHz.
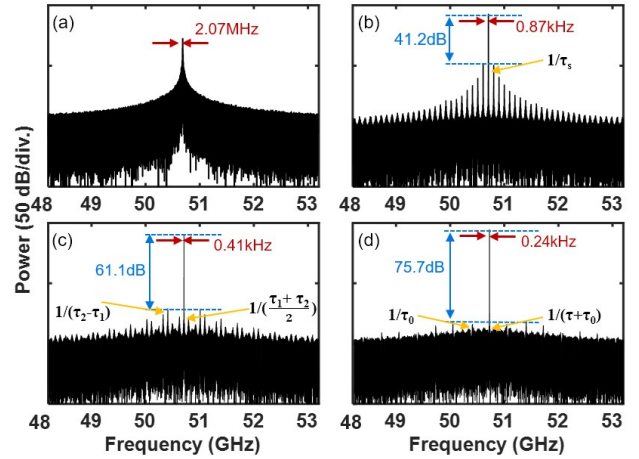

Fig. 6 Numerical simulation of the power spectra of the optically injected DM laser output (a) without feedback, (b) with single optical feedback, (c) with double optical feedback, (d) with photonic filter feedback.

The numerically simulated power spectra of the generated mmWave are displayed in Fig. 6. For comparison, Fig. 6(a)-(d) show the generated mmWave power spectra without optical feedback and with single, double, and photonic filter feedback, respectively. The injection strength and the frequency detuning are fixed at 130 ns^{-1} and 50 GHz, respectively. At these parameters, the optically injected DM laser operates at P1 oscillation with the oscillation frequency of about 50 GHz. As shown in Fig. 6(a), without optical feedback, the linewidth of the generated mmWave signal is 2.07 MHz. The fundamental frequency is about 50.7 GHz due to the weak red-shift effect on cavity frequency when the frequency detuning is large [16]. Fig. 6(b) gives the power spectrum of the generated mmWave signal with single optical feedback. The feedback strength η_s is set at 1.5 ns^{-1} to avoid undesirable dynamics change, and the feedback delay time τ_s is 10 ns. Apparently, the introduction of single optical feedback helps to reduce the mmWave linewidth to 0.87 kHz, and the peak power at the fundamental frequency is also enhanced. However, the external optical feedback also introduces obvious side peaks adjacent to the central peak. The interval is nearly 100 MHz, which corresponds to the reciprocal

of the feedback delay time τ_s. Next, the double optical feedback scheme is applied, and the corresponding mmWave power spectrum is shown in Fig. 6(c). To optimize the mmWave linewidth and SPS ratio, the optical feedback parameters are set as $\eta_1 = \eta_2 = 1/2\eta_s = 0.75$ ns^{-1}, $\tau_1 = 10$ ns, $\tau_2 = 13$ ns. As a result, the linewidth of the generated mmWave is reduced by about 50%, and the SPS ratio increases to 61.1 dB, which is about 20 dB enhancement compared with that of the single feedback case. Whereas the residual side peaks can still be observed, which can be classified into two types. One type contains the peaks at a frequency interval of about 83.7 MHz, which corresponds to the reciprocal of the averaged feedback delay $(\tau_1+\tau_2)/2$, the other type contains the peaks at a frequency interval of about 300 MHz, which corresponds to the reciprocal of the difference between τ_1 and τ_2. Moreover, the power of the first side peak resulting from the time delay difference between the dual feedback loops is higher than those corresponding to the averaged external feedback delay time, which indicates, under this feedback strength level, the frequency beating effect of the two external cavity modes is the main impact factor for the SPS ratio. Finally, the power spectrum of the generated mmWave signal subject to photonic filter feedback is illustrated in Fig. 6(d). The feedback parameters are set as, $\eta = 1.5$ ns^{-1}, $r = 0.1$, $\tau = 10$ ns, and $\tau_0 = 3$ ns. We can find that the linewidth of the central peak further reduces to 0.24 kHz, and the SPS ratio is 75.7 dB, which has about 15 dB improvement compared with that of the double feedback case. The residual side peaks become contiguous, smooth, and hardly be identified. Further studies demonstrate that the interval between the small ripples are about 78 MHz and 314.2 MHz, which are correspond to the reciprocal of $\tau + \tau_0$ and τ_0, as indicated in Fig. 6(d). In general, the simulation results are in qualitative agreement with our experimental observations that the photonic filter feedback scheme has superiority in terms of reduced linewidth and side peaks suppression of the generated mmWave compared to single and double optical feedback schemes.
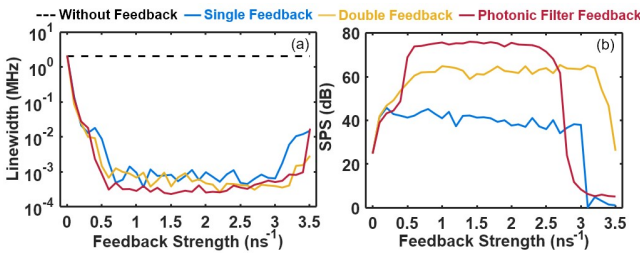

Fig. 7 Numerical simulation of the photonic millimeter wave linewidth (a), side peak suppression ratio (b) as a function of optical feedback strength.

The effect of the optical feedback strength on the linewidth and SPS ratio of the generated mmWave signal is studied and shown in Fig. 7. The results of the single and double optical feedback schemes are also plotted for comparison. The optical feedback strength is set as $\eta = \eta_s = 2\eta_1 = 2\eta_2$, and other optical feedback parameters are the same as the cases in Fig. 6. The variation of the mmWave linewidth with the feedback strength is shown in Fig. 7(a). We can see that the linewidth evolution caused by the three optical feedback schemes has a similar trend. The linewidth of the generated mmWave first rapidly narrows with the increase of the feedback strength until the feedback strength reaches around 0.6 ns^{-1}, then the linewidth remains basically the same except for small fluctuations until the feedback strength increases to around 3 ns^{-1}. Further increasing the feedback strength, the linewidth increases again. The results show that all three optical feedback schemes can narrow the linewidth to around 1kHz, and the performance of the three feedback schemes in terms of linewidth reduction is comparable. But as shown in Fig. 7(b), the outstanding advantage of the photonic filter feedback scheme is to enhance the SPS ratio. For $\eta < 0.5$ ns^{-1}, the SPS ratio of the photonic filter feedback increases with the feedback strength, which is a result of the significant increase in the peak power of the fundamental frequency and the less pronounced external cavity modes when the photonic filter feedback is introduced. For 0.6 ns$^{-1} < \eta < 2.4$ ns^{-1}, the generated mmWave signal can maintain a SPS ratio of about 75dB, which is about 15dB (35dB) higher than that of double (single) optical feedback schemes. The numerically simulated results qualitatively agree with the experimental observation in Fig. 3.

To further explore the distinctive SPS performance of the photonic filter feedback scheme, the map of SPS ratio in the parameter space of the coupling coefficient as well as the phase variables in the ring cavity is plotted in Fig. 8. The feedback strength is fixed at a medium level with $\eta = 1.5$ ns^{-1}. As shown in Fig. 8, for in-phase optical feedback ($\varphi = 0$), with the increase of the coupling coefficient, the SPS ratio gradually decreases but is still higher than 60 dB when $r = 0.9$, which is close to the maximum SPS ratio that can be achieved with a double feedback scheme. The result shows that a low coupling coefficient is beneficial to obtain a higher SPS ratio. This is because a lower coupling coefficient means more optical power is split into the ring cavity of the photonic filter, thus the relatively strong multiple Vernier effect can help vanish residual side peaks induced by the external cavity modes, and effectively increase the SPS ratio. This result is consistent with our experimental results. In addition, the SPS performance of the photonic filter feedback scheme under the feedback strength is less sensitive to the phase change in the ring cavity as the free spectral range of each ring cavity recirculation can still match each other following Vernier principle [42].
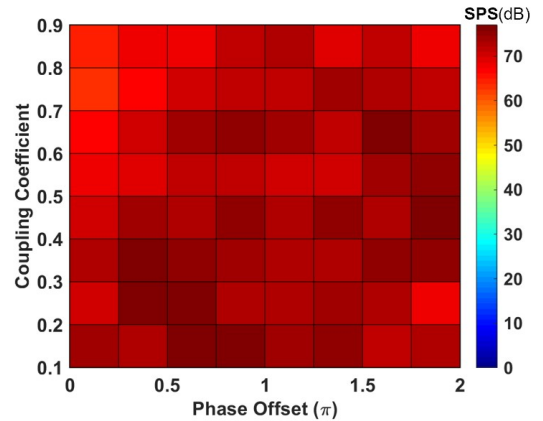

Fig. 8 Simulation of the side peak suppression ratio as a map of phase offset and coupling coefficient.

IV. Conclusions

In summary, the photonic millimeter wave generation and stabilization based on P1 dynamic of an optically injected DM semiconductor laser with photonic filter feedback are theoretically investigated and experimentally demonstrated. The results show that >30 GHz mmWave can be obtained based on P1 oscillation of the DM laser under suitable optical injection. In addition, a photonic filter is introduced in the optical feedback loop to optimize the quality of the generated mmWave. The results demonstrate that compared with single/double optical feedback configurations, the photonic filter feedback scheme has a superior performance in improving SPS ratio and stability, and has a comparable performance in linewidth reduction. Further numerical simulation results demonstrate that for the photonic filter feedback, multiple Vernier effect in the ring cavity is beneficial for enhancing the SPS ratio, thus a low coupling coefficient, meaning more optical feedback power propagated in the ring cavity, is preferred. The numerical analytical results are qualitatively in agreement with the experimental results. This work will help to understand the stabilization mechanism of photonic filter feedback and contribute to the generation of high frequency, narrow linewidth, and high stability photonic millimeter wave signals.

References

[1] L. Kong, M. K. Khan, F. Wu, G. Chen, and P. Zeng, "Millimeter-Wave Wireless Communications for IoT-Cloud Supported Autonomous Vehicles: Overview, Design, and Challenges," *IEEE Commun. Mag.*, vol. 55, no. 1, pp. 62–68, 2017.

[2] X. Li, J. Yu, and G. K. Chang, "Photonics-Aided Millimeter-Wave Technologies for Extreme Mobile Broadband Communications in 5G," *J. Light. Technol.*, vol. 38, no. 2, pp. 366–378, 2020.

[3] S. Ju, Y. Xing, O. Kanhere, and T. S. Rappaport, "Millimeter Wave and Sub-Terahertz Spatial Statistical Channel Model for an Indoor Office Building," *IEEE J. Sel. Areas Commun.*, vol. 39, no. 6, pp. 1561–1575, 2021.

[4] X. Shen, Y. Liu, L. Zhao, G. L. Huang, X. Shi, and Q. Huang, "A Miniaturized Microstrip Antenna Array at 5G Millimeter-Wave Band," *IEEE Antennas Wirel. Propag. Lett.*, vol. 18, no. 8, pp. 1671–1675, 2019.

[5] D. Wake, C. R. Lima, and P. A. Davies, "Optical Generation of Millimeter-wave Signals for Fiber-radio Systems using a Dual-mode DFB Semiconductor Laser," *IEEE Trans. Microw. Theory Tech.*, vol. 43, no. 9, pp. 2270–2276, 1995.

[6] C. T. Tsai, C. H. Lin, C. T. Lin, Y. C. Chi, and G. R. Lin, "60-GHz Millimeter-wave Over Fiber with Directly Modulated Dual-mode Laser Diode," *Sci. Rep.*, vol. 6, no. 1, pp. 27919, 2016.

[7] E. A. Kittlaus, D. Eliyahu, S. Ganji, S. Williams, A. B. Matsko, K. B. Cooper, and S. Forouhar, "A Low-noise Photonic Heterodyne Synthesizer and Its Application to Millimeter-wave Radar," *Nat. Commun.*, vol. 12, no. 1, pp. 4397, 2021.

[8] K. Zeb, J. Liu, Y. Mao, G. Liu, P. J. Poole, M. Rahim, G. Pakulski, P. Barrios, M. Vachon, D. Poitras, W. Jiang, J. Weber, X. Zhang, and J. Yao, "Broadband Optical Heterodyne Millimeter-wave-over-fiber Wireless Links Based on a Quantum Dash Dual-Wavelength DFB Laser," *J. Light. Technol.*, vol. 40, no. 12, pp. 3698–3708, 2022.

[9] W. Liu, Y. Huang, Y. Sun, A. Wang, Y. Qin, and Y. Wang, "Broadband and Flat Millimeter-wave Noise Source based on the Heterodyne of Two Fabry–Perot Lasers," *Opt. Lett.*, vol. 47, no. 3, pp. 541–544, 2022.

[10] S. K. Hwang, S. C. Chan, S. C. Hsieh, and C. Y. Li, "Photonic Microwave Generation and Transmission Using Direct Modulation of Stably Injection-locked Semiconductor Lasers," *Opt. Commun.*, vol. 284, no. 14, pp. 3581–3589, 2011.

[11] L. Wang, G. Li, T. Hao, S. Zhu, M. Li, N. Zhu, and W. Li, "Photonic Generation of Multiband and Multi-format Microwave Signals Based on a Single Modulator," *Opt. Lett.*, vol. 45, no. 22, pp. 6190–6193, 2020.

[12] Z. Deng and J. Yao, "Photonic Generation of Microwave Signal Using a Rational Harmonic Mode-locked Fiber Ring Laser," *IEEE Trans. Microw. Theory Tech.*, vol. 54, no. 2, pp. 763–767, 2006.

[13] G. K. M. Hasanuzzaman, S. Iezekiel, and A. Kanno, "W-Band Optoelectronic Oscillator," *IEEE Photonics Technol. Lett.*, vol. 32, no. 13, pp. 771–774, 2020.

[14] Z. Fan, W. Zhang, Q. Qiu, and J. Yao, "Hybrid Frequency-Tunable Parity-Time Symmetric Optoelectronic Oscillator," *J. Light. Technol.*, vol. 38, no. 8, pp. 2127–2133, 2020.

[15] M. Li, T. Hao, W. Li, and Y. Dai, "Tutorial on Optoelectronic Oscillators," *APL Photonics*, vol. 6, no. 6, pp. 061101, 2021.

[16] M. AlMulla and J. M. Liu, "Linewidth Characteristics of Period-one Dynamics Induced by Optically Injected Semiconductor Lasers," *Opt. Express*, vol. 28, no. 10, pp. 14677–14693, 2020.

[17] J. P. Zhuang and S. C. Chan, "Tunable Photonic Microwave Generation Using Optically Injected Semiconductor Laser Dynamics with Optical Feedback Stabilization," *Opt. Lett.*, vol. 38, no. 3, pp. 344–346, 2013.

[18] P. Zhou, N. Li, and S. Pan, "Period-One Laser Dynamics for Photonic Microwave Signal Generation and Applications," *Photonics*, vol. 9, no. 4, pp. 227, 2022.

[19] J. P. Zhuang, X. Z. Li, S. S. Li, and S. C. Chan, "Frequency-modulated Microwave Generation with Feedback Stabilization Using an Optically Injected Semiconductor Laser," *Opt. Lett.*, vol. 41, no. 24, pp. 5764–5767, 2016.

[20] T. B. Simpson and F. Doft, "Double-locked Laser Diode for Microwave Photonics Applications," *IEEE Photonics Technol. Lett.*, vol. 11, no. 11, pp. 1476–1478, 1999.

[21] L. Fan, G. Xia, J. Chen, X. Tang, Q. Liang, and Z. Wu, "High-purity 60GHz Band Millimeter-wave Generation Based on Optically Injected Semiconductor Laser Under Subharmonic Microwave Modulation," *Opt. Express*, vol. 24, no. 16, pp. 18252–18265, 2016.

[22] K. H. Lo, S. K. Hwang, and S. Donati, "Optical Feedback Stabilization of Photonic Microwave Generation Using Period-one Nonlinear Dynamics of Semiconductor Lasers," *Opt. Express*, vol. 22, no. 15, pp. 18648–18661, 2014.

[23] J. P. Zhuang and S. C. Chan, "Phase Noise Characteristics of Microwave Signals Generated by Semiconductor Laser Dynamics," *Opt. Express*, vol. 23, no. 3, pp. 2777–2797, 2015.

[24] S. Ji, C. Xue, A. Valle, P. S. Spencer, H. Li, and Y. Hong, "Stabilization of Photonic Microwave Generation in Vertical-Cavity Surface-Emitting Lasers With Optical Injection and Feedback," *J. Light. Technol.*, vol. 36, no. 19, pp. 4347–4353, 2018.

[25] X. W. Ma, Y. Z. Huang, L. X. Zou, B. W. Liu, H. Long, H. Z. Weng, Y. D. Yang, and J. L. Xiao, "Narrow-linewidth Microwave Generation Using AlGaInAs/InP Microdisk Lasers subject to Optical Injection and Optoelectronic Feedback," *Opt. Express*, vol. 23, no. 16, pp. 20321–20331, 2015.

[26] J. S. Suelzer, T. B. Simpson, P. Devgan, and N. G. Usechak, "Tunable, Low-phase-noise Microwave Signals from an optically Injected Semiconductor Laser with Opto-electronic Feedback," *Opt. Lett.*, vol. 42, no. 16, pp. 3181–3184, 2017.

[27] Y. H. Hung and S. K. Hwang, "Photonic Microwave Stabilization for Period-one Nonlinear Dynamics of Semiconductor Lasers using Optical Modulation Sideband Injection Locking," *Opt. Express*, vol. 23, no. 5, pp. 6520–6532, 2015.

[28] C. H. Tseng, C. T. Lin, and S. K. Hwang, "V- and W-band Microwave Generation and Modulation Using Semiconductor Lasers at Period-one Nonlinear Dynamics," *Opt. Lett.*, vol. 45, no. 24, pp. 6819–6822, 2020.

[29] S. Osborne, S. O'Brien, K. Buckley, R. Fehse, A. Amann, J. Patchell, B. Kelly, D. R. Jones, J. O'Gorman, and E. P. O'Reilly, "Design of Single-Mode and Two-Color Fabry–PÉrot Lasers with Patterned Refractive Index," *IEEE J. Sel. Top. Quantum Electron.*, vol. 13, no. 5, pp. 1157–1163, 2007.

[30] N. Oliver, M. C. Soriano, D. W. Sukow, and I. Fischer, "Fast Random Bit Generation Using a Chaotic Laser: Approaching the Information Theoretic Limit," *IEEE J. Quantum Electron.*, vol. 49, no. 11, pp. 910–918, 2013.

[31] A. Campos-Mejía, A. N. Pisarchik, and D. A. Arroyo-Almanza, "Noise-induced on–off Intermittency in Mutually Coupled Semiconductor Lasers," *Chaos Solitons Fractals*, vol. 54, pp. 96–100, 2013.

[32] A. Rosado, A. Pérez-Serrano, J. M. G. Tijero, A. V. Gutierrez, L. Pesquera,

and I. Esquivias, "Numerical and Experimental Analysis of Optical Frequency Comb Generation in Gain-Switched Semiconductor Lasers," *IEEE J. Quantum Electron.*, vol. 55, no. 6, pp. 1–12, 2019.

[33] D. Chang, Z. Zhong, J. Tang, P. S. Spencer, and Y. Hong, "Flat Broadband Chaos Generation in a Discrete-mode Laser Subject to Optical Feedback," *Opt. Express*, vol. 28, no. 26, pp. 39076–39083, 2020.

[34] Z. Q. Zhong, D. Chang, W. Jin, M. W. Lee, A. Wang, S. Jiang, J. He, J. Tang and Y. Hong, "Intermittent Dynamical State Switching in Discrete-mode Semiconductor Lasers Subject to Optical Feedback," *Photonics Res.*, vol. 9, no. 7, pp. 1336–1342, 2021.

[35] D. Chang, Z. Q. Zhong, A. Valle, W. Jin, S. Jiang, J. Tang, and Y. Hong, "Microwave Photonic Signal Generation in an Optically Injected Discrete Mode Semiconductor Laser," *Photonics*, vol. 9, no. 3, pp. 171, 2022.

[36] A. Valle, "Statistics of the Optical Phase of a Gain-Switched Semiconductor Laser for Fast Quantum Randomness Generation," *Photonics*, vol. 8, no. 9, pp. 388, 2021.

[37] J. Capmany, B. Ortega, and D. Pastor, "A Tutorial on Microwave Photonic Filters," *J. Light. Technol.*, vol. 24, no. 1, pp. 201–229, 2006.

[38] M. Yu, H. Wang, and Y. Ji, "Investigation on The Complex and Tunable Laser Chaos Generated by The Microresonator Optical Combs Injection," *IEEE J. Sel. Top. Quantum Electron.*, vol. 29, no. 1, pp. 0600110, 2023.

[39] N. Jiang, Y. Wang, A. Zhao, S. Liu, Y. Zhang, L. Chen, B. Li, and K. Qiu, "Simultaneous Bandwidth enhanced and Time Delay Signature suppressed Chaos Generation in Semiconductor Laser Subject to Feedback from Parallel Coupling Ring Resonators," *Opt. Express*, vol. 28, no. 2, pp. 1999–2009, 2020.

[40] A. Wang, Y. Wang, Y. Yang, M. Zhang, H. Xu, and B. Wang, "Generation of Flat-spectrum Wideband Chaos by Fiber Ring Resonator," *Appl. Phys. Lett.*, vol. 102, no. 3, pp. 031112, 2013.

[41] V. V. Spirin, J. L. Bueno Escobedo, D. A. Korobko, P. Mégret, and A. A. Fotiadi, "Stabilizing DFB Laser Injection-locked to an External Fiber-optic Ring Resonator," *Opt. Express*, vol. 28, no. 1, pp. 478–484, 2020.

[42] O. Pottiez, O. Deparis, R. Kiyan, M. Haelterman, P. Emplit, P. Megret, and M. Blondel, "Supermode Noise of Harmonically Mode-locked Erbium Fiber Lasers with Composite Cavity," *IEEE J. Quantum Electron.*, vol. 38, no. 3, pp. 252–259, 2002.

[43] J. Dellunde, M. C. Torrent, J. M. Sancho, and M. San Miguel, "Frequency Dynamics of Gain-switched Injection-locked Semiconductor Lasers," *IEEE J. Quantum Electron.*, vol. 33, no. 9, pp. 1537–1542, 1997.

[44] C. Xue, S. Ji, Y. Hong, N. Jiang, H. Li, and K. Qiu, "Numerical Investigation of Photonic Microwave Generation in an Optically Injected Semiconductor Laser subject to Filtered Optical Feedback," *Opt. Express*, vol. 27, no. 4, pp. 5065–5082, 2019.